

# Controlling entanglement in InGaAs/GaAs quantum dot molecules via electric fields

Gabriel Bester and Alex Zunger

National Renewable Energy Laboratory, Golden CO 80401

(Dated: December 2, 2024)

The degree of entanglement of excitons in vertically coupled, self-assembled InGaAs quantum dots is shown to be tunable by an external electric field applied in growth direction. Using atomistic pseudopotential calculations followed by a configuration interaction many-body treatment of correlations, we calculate the electronic states, degree of entanglement and optical absorption. We offer a novel way to spectroscopically identify the magnitude of electric field needed to maximize the entanglement.

PACS numbers: 78.67.Hc, 73.21.La, 03.67.Mn

A pair of quantum dots or “quantum dot molecule” (QDM) occupied by two electrons [1, 2] or by an electron-hole pair [3] have been offered [1, 2, 3] as a basis for quantum computing. The fundamental requirement for such quantum algorithm is the availability of entangled states and the ability to entangle and disentangle the quantum bits (qubits). In the context of a dot molecule, an entangled electron-hole pair can be represented by the the maximally entangled Bell state  $e_T h_T + e_B h_B$ , where  $e$  and  $h$  stand for the electron and the hole (the two qubits) and  $T$  and  $B$  for their localizations in top or bottom dot. The original proposal [3] and subsequent experiments [3, 4, 5] for entangled electron-hole pairs in QDMs promised a *high* degree of entanglement [3] based on analysis via simple models. However, later theoretical work showed [6] that excitonic entanglement is generally low in such cases and develops a sharp maximum only at a critical interdot separation. Unfortunately, it has proven to be difficult to experimentally control so precisely the interdot distance in a QDM, zooming to the point of maximum entanglement. The question we address here is whether the degree of entanglement can be maximized by other means, more accessible experimentally than a variation of the interdot separation. We propose and quantify theoretically that it is possible to *tune* and control the degree of entanglement by applying an external electric field in the growth direction [7, 8, 9, 10]: While the entanglement at zero field is around 35%, it reaches around 75% at an electric field of  $F_{Smax} = -5.4$  kV/cm. Moreover, precisely at this field the first two excitons merge, giving a well defined spectroscopic signature of the point of maximal entanglement.

We solve the Schrödinger equation with the Hamiltonian  $H = -1/2\nabla^2 + \sum_{\alpha,n} v_{\alpha}(\mathbf{r} - \mathbf{R}_n) + V_{SO} + |e|Fz$  under an external electric field  $F$  applied in [001] ( $z$ ) direction. The atomistic pseudopotentials  $v_{\alpha}$  of atom of type  $\alpha$  and the non-local spin-orbit potential  $V_{SO}$  are fit to reproduce InAs and GaAs bulk properties [6, 11]. The atomic positions  $\{\mathbf{R}_n\}$  are obtained by minimizing the atomistic strain energy (via valence force field [12]) for a given shape and size of the dots. Our quantum dots have a truncated cone shape (12 nm base and 2 nm height) with a composition ranging from pure InAs at the top to  $\text{In}_{0.5}\text{Ga}_{0.5}\text{As}$  at the

base as determined in Ref. [3]. The single-particle Hamiltonian is diagonalized in a basis  $\Psi = \sum_{n,k} A_{n,k} \phi_{n,k}$  of pseudopotential Bloch functions  $\phi_{n,k}$  as outlined in Ref. 13. Correlations are treated via a many-body expansion in Slater determinants [14, 15] where the electrons not included dynamically are represented by a model screening of the Coulomb and (long and short range) exchange [16]. The entanglement is calculated according to the von Neumann entropy of entanglement [17, 18].

The bonding ( $b$ ) and antibonding ( $a$ ) electron molecular levels of a dot molecule will be denoted as  $E_a, E_b$ . For an idealized symmetric case the lowest energy molecular orbitals (MOs) develop from single-dot electron states  $e_T$  and  $e_B$  located on the bottom ( $B$ ) and top ( $T$ ) dots:

$$\psi[E_b] = \frac{1}{\sqrt{2}}(e_T + e_B); \quad \psi[E_a] = \frac{1}{\sqrt{2}}(e_T - e_B), \quad (1)$$

and similarly for the holes  $H_a, H_b$ . As shown previously [6, 19], in reality, because of strain and random-alloy fluctuations, one does not have a *symmetric* bonding-antibonding behavior even if the dot molecule is made of identical (but non-spherical) dots. This is seen in Fig. 1 where both electron and hole molecular orbital wave functions are shown for zero electric field  $F = 0$ . We see that the (lighter-mass) electrons tunnel between dots, forming bonding-antibonding states as in Eq. (1), but the (heavier-mass) holes remain localized on the top (bottom) dot for the bonding (antibonding) MO  $H_b$  ( $H_a$ ). The single-particle molecular orbital energy levels are shown in Fig. 2. As we apply an electric field the molecular levels that develop from the single-dot orbitals exhibit anti-crossing. We have indicated in Fig. 2 the major character of the molecular states  $E_a, E_b, H_a, H_b$  in terms of the localization on individual dots ( $e_T, e_B, h_T$  and  $h_B$ ) using the calculated MO wave functions of Fig. 1. We see that for holes at positive fields  $\psi(H_a) \simeq h_T$  and  $\psi(H_b) \simeq h_B$  while for electrons  $\psi(E_a) \simeq e_T$  and  $\psi(E_b) \simeq e_B$ . The opposite is true for negative fields. Thus, by applying an electric field we can tune the localization of the MO's. In real diatomic molecules ( $H_2, N_2, \dots$ ) this would require unrealistically high fields. We will see that this tuning of localization will also control the degree of entanglement.

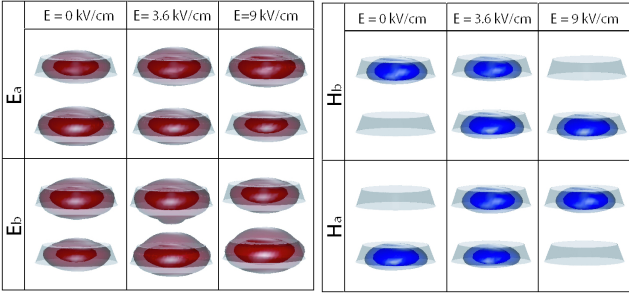


FIG. 1: Square of the first two electron and first two hole wave functions of an InGaAs/GaAs quantum dot as a function of electric field at an interdot separation  $d=7.9$  nm.

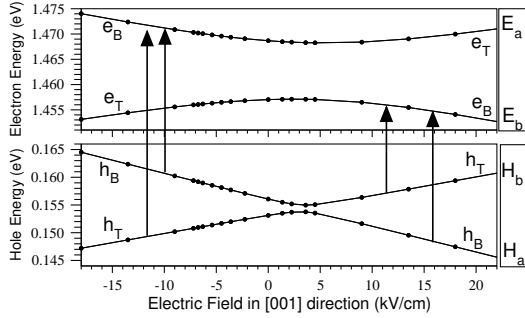


FIG. 2: Single particle electron (upper panel) and hole (lower panel) eigenvalues as a function of electric field for  $d=7.9$  nm with respect to the GaAs valence band maximum. We indicate the localization of the MOs on top and bottom dot by  $e_T$ ,  $e_B$ ,  $h_T$ ,  $h_B$ .

There are four transitions between the four molecular levels shown as vertical arrows in Fig. 2. Their single-particle transition energies  $\varepsilon_g^{i,j}$  (differences between the energies from Fig. 2) are given in Fig. 3(a) and show maxima and minima vs field. We note in Fig. 3(a) the character of the four transitions in terms of localization on single-dot orbitals. We see that at high fields, the lowest- and highest-energy transitions involve *different* dots: for example  $E_b H_b$  is  $e_B h_T$  at positive field, and  $e_T h_B$  at negative field. Thus, the corresponding dipole transitions are expected to be weak (“dark states”). In contrast the second and third transitions at high fields involve the *same* dots: for example  $E_b H_a$  is  $e_B h_B$  at positive fields and  $e_T h_T$  at negative field. Thus, the corresponding dipole transitions are expected to be large (“bright states”).

The single-particle approximation underlying Fig. 3(a) is valid only in the case of large fields, where e-h Coulomb effects are small compared to the field-driven variation in the single-particle levels. At these large fields, the excitons are pure determinants with localization on either  $e_T h_T$  or  $e_T h_B$  or  $e_B h_T$  or  $e_B h_B$  and therefore show no entanglement. We will next see that in the interesting region of electric fields, e-h Coulomb interactions are crucial. In Figure 3(b) we show the calculated electron-hole Coulomb inter-

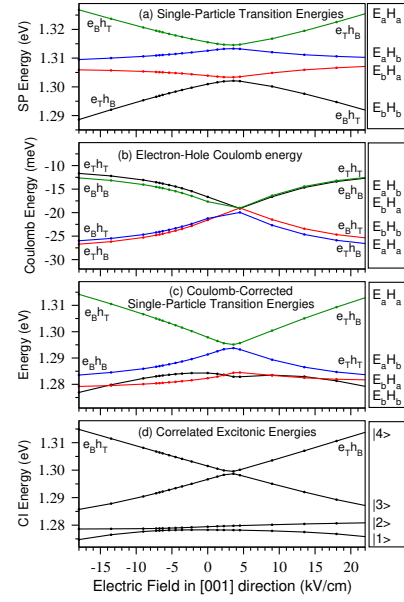


FIG. 3: (Color) Transition energies for  $d=7.9$  nm as a function of electric field in different approximations: (a) Single particle transition energies (b) Direct electron-hole Coulomb matrix elements between MOs. (c) Transition energies including electron-hole Coulomb interaction:  $\varepsilon_g^{i,j} - J_{e,h}^{i,j}$ , but without correlation effects. (d) Final correlated exciton results. The bidot products ( $e_T h_T$ , etc...) are given whenever the MO states (given on the right) are strongly dominated by one of these products.

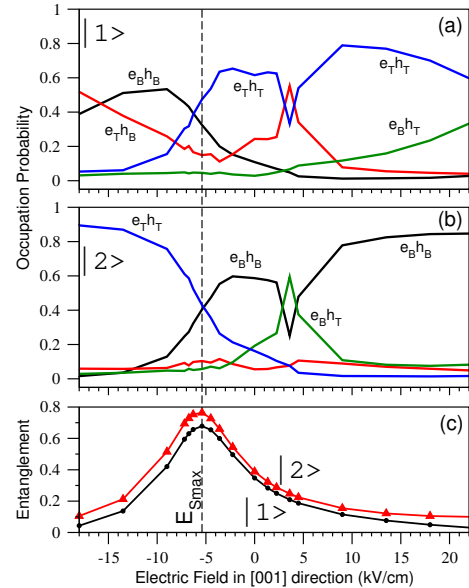


FIG. 4: Occupation probabilities given as the bidot products  $e_T h_T$  or  $e_T h_B$  or  $e_B h_T$  and  $e_B h_B$  as a function of the electric field for the first two exciton states  $|1\rangle$  (a) and  $|2\rangle$  (b) for  $d=7.9$  nm. (c) Entropy of entanglement of the first two excitons.

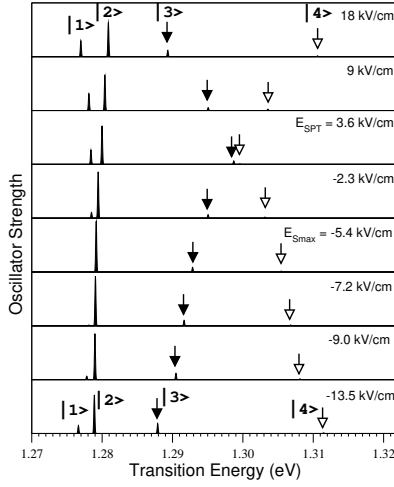


FIG. 5: Oscillator strength of the first four transitions (first 16 transitions including spin) as a function of electric field for  $d=7.9$  nm.)

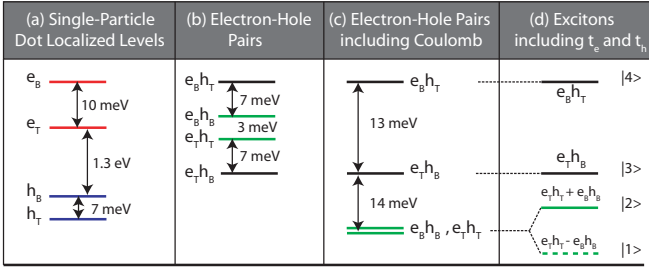


FIG. 6: Formation of the highly entangled excitonic states at the critical field  $F=-5.4$  kV/cm. (a) Single particle electron and hole levels in the dot-localized basis. (b) Simple differences between the single particle electron and hole energies from (a). (c) Adding electron-hole direct Coulomb interaction to (b). (d) Adding electron and hole hopping the the levels from (c)

action

$$J_{e,h}[i-j] = \iint \frac{\psi_i^*(\mathbf{r}_a)\psi_j^*(\mathbf{r}_b)\psi_j(\mathbf{r}_b)\psi_i(\mathbf{r}_a)}{\epsilon(\mathbf{r}_a, \mathbf{r}_b)|\mathbf{r}_a - \mathbf{r}_b|} d\mathbf{r}_a d\mathbf{r}_b \quad (2)$$

between the MOs ( $i = E_a$  or  $E_b$ ) and ( $j = H_a$  or  $H_b$ ) using the model of Resta [16] for the screening  $\epsilon$ . This interaction  $J_{e,h}$  shows the reverse behavior vs field compared with the MO energies  $\epsilon_g$  vs field [Fig. 3(a)]. For example, whereas  $J_{e,h}[E_b H_b]$  is *minimal* at large positive or negative fields, and *maximal* at intermediate fields, the MO band gap  $\epsilon_g[E_b H_b]$  is *minimal* at large positive or negative fields and *maximal* at intermediate fields. Not surprisingly, when one calculates the Coulomb-corrected excitonic transition energy  $\epsilon_g^{i,j} - J_{e,h}^{i,j}$  between the molecular states  $i$  and  $j$  [Fig. 3(c)] one sees a partial cancellation for the two low-energy transitions,  $E_b H_b$  and  $E_b H_a$ , leading to a weak dependence of the transition energy on field. In contrast, inspection of Figs. 3(a) and 3(b) for the two

highest-energy transitions shows that the field-dependence of  $\epsilon_g^{i,j}$  and  $J_{e,h}^{i,j}$  reinforce each other, so the excitonic gap  $\epsilon_g^{i,j} - J_{e,h}^{i,j}$  [Fig. 3(c)] has an *amplified* dependence on field. We conclude that the combination of  $\epsilon_g$  and  $J_{e,h}$  brings the lowest-energy transitions *closer* to each other, while pushing the two higher-energy transitions *apart*. This will affect the correlation coupling between the MO's, as seen next.

The Coulomb-corrected excitonic transition energies  $\epsilon_g^{i,j} - J_{e,h}^{i,j}$  neglect the interactions between the different configurations, i.e., the states from Fig. 3(c) are not allowed to interact. This interaction is included in the next step via a configuration interaction (CI)[14, 15] calculation in which we include all Coulomb and exchange integrals from the first four electron and first four hole states (including spin). The results are shown in Fig. 3(d) as a function of electric field. The lowest energy transitions (excitons |1> and |2>) have a very weak dependence on field, similarly to the case without correlations [Fig. 3(c)]. In contrast to the perturbative approach of Fig. 3(c) the states do not cross but anticrossing at  $-5.4$  kV/cm, as expected from interacting states. Similarly, |3> and |4> anticross at  $+3.6$  kV/cm but in a more abrupt fashion.

To understand the correlated CI results we next analyze |1>, |2>, |3>, |4> by decomposing the correlated excitonic states into sums of products of single-dot states  $e_T h_T$ ,  $e_B h_T$ ,  $e_T h_B$  and  $e_B h_B$  called “bidot products” (see Ref. 18 for details). The results of this decomposition are given in Fig. 4(a)(b) for states |1> and |2> as a function of the electric field. We see that the exciton |1> is composed of many bidot-products over the complete range of fields studied. In the case of very strong positive fields (larger than 20 kV/cm), state |1> is purely  $e_B h_T$  (unentangled), as the field pulls the electron to the bottom dot and the hole to the top dot. The excitons |2> and |3> are already, at moderate positive fields, purely  $e_B h_B$  and  $e_T h_T$  and remain like this at large field. Fig. 4(c) shows the degree of entanglement calculated for the correlated CI wave functions using the von Neumann formula [6, 17]  $S = -\text{Tr} \rho_e \log_2 \rho_e$ , where  $\rho_e$  is the reduced density matrices of the electron. The entanglement of |1> and |2> reaches its maximum of around 75% at  $F_{Smax} = -5.4$  kV/cm. At this field the exciton states |1> and |2> are mainly composed of  $e_T h_T$  and  $e_B h_B$  configurations, as shown in Fig. 4(a)(b). The high degree of entanglement is reached when certain “resonant conditions”, manifested by the anti-crossing in Fig. 5 and Fig. 3(d), are reached. This can be understood from Fig. 6 that uses exclusively the language of dot-localized orbitals (as opposed to MO's). We therefore rotate the MO's until the on-site Coulomb interaction is maximized. This procedure is used to build maximally localized Wannier functions [20] and allows us to calculate the single-particle energies of the dot-localized orbitals, denoted as  $e_T$ ,  $e_B$ ,  $h_T$  and  $h_B$  in Fig. 6(a). Note, that these orbitals, unlike the MO's, do not include any hopping terms since they are purely localized on one of the two dots. The hopping terms will play an

important role later in the discussion. Figure 6 describes the situation at  $F_{Smax}$ . Fig. 6(a) shows that the energies of the dot-localized electron and hole orbitals are separated by 10 and 7 meV respectively with a gap of 1.3 eV. Fig. 6(b) shows the energies of simple products of these electron and hole states. They show two closely spaced levels (3 meV apart) in the center of the spectrum and two states 7 meV lower and higher in energy. These energies are different from the MO's energies of Fig. 3(a) that are combinations of  $e_T h_T$ ,  $e_T h_B$ ,  $e_B h_T$  and  $e_B h_B$  at this field. In the next step, in Fig. 6(c), the two-body Coulomb attraction is taken into account and lowers the  $e_T h_T$  and  $e_B h_B$  states in such a way that they are about 14 meV below the  $e_T h_B$  state. This is the consequence of a weak e-h binding for the dissociated excitons  $e_T h_B$  and  $e_B h_T$ . Notably, the simple products  $e_T h_T$  and  $e_B h_B$  are energetically nearly *degenerate* at this level, this is the “resonant condition” mentioned above. In the last step, in Fig. 6(d), the excitons  $|1\rangle$  and  $|2\rangle$  are now created by including the effects of electron and hole hopping that effectively produce correlated states. The excitons  $|1\rangle$  and  $|2\rangle$  are now a bonding- and antibonding-like combination of the energetically degenerate  $e_T h_T$  and  $e_B h_B$  states. The excitons  $|1\rangle$  and  $|2\rangle$  are now split by a small energy of less than 1 meV. This small splitting is conceptually very similar to the Davydov splitting [21] in molecular crystals. Importantly, these combinations are highly symmetric and anti-symmetric, leading to maximal degree of entanglement. The analysis also reveals that exciton  $|1\rangle$  is anti-symmetric ( $e_T h_T - e_B h_B$ ) and therefore optically dark. Exciton  $|2\rangle$  is symmetric ( $e_T h_T + e_B h_B$ ) and made from bidot products where electron and hole have large overlap and is therefore optically bright. For deviations from  $F_{Smax}$ , the states  $e_T h_T$  and  $e_B h_B$  get out of resonance and form less symmetric combinations (with lower entanglement and smaller oscillator strength) as  $\frac{1}{\sqrt{2}}(\alpha e_T h_T + \beta e_B h_B)$  with  $\alpha \neq \beta$ . This is a similar case to the bonding and antibonding states of ionic heteronuclear dimers.

The calculated excitonic states of Fig. 3(d) are finally used to calculate the absorption spectra (Fig. 5). The spectra shows that at the anticrossings of  $|1\rangle$  and  $|2\rangle$  the lowest exciton  $|1\rangle$  is dark and progressively gains oscillator strength over a large electric field range away from the anticrossing.

We showed that the degree of excitonic entanglement in vertically coupled self-assembled quantum dots can be tuned by an external electric field and that the point of maximum entanglement can be identified by measuring the photoluminescence spectra, observing the merging of two

peaks. We consequently analyze the nature of the excitons and reveal the interplay of single particle effects, direct Coulomb binding and electron and hole hopping on the many body levels. We describe how these effects conspire to yield a highly entangled state.

This work was supported by the US Department of Energy (OS/BES) under the LAB 03-17 initiative.

- 
- [1] D. P. DiVincenzo, *Science* **270**, 255 (1995).
  - [2] D. Loss and D. P. DiVincenzo, *Phys. Rev. A* **57**, 120 (1998).
  - [3] M. Bayer, P. Hawrylak, K. Hinzer, S. Fafard, M. Korkusinski, Z. R. Wasilewski, O. Stern, and A. Forchel, *Science* **291**, 451 (2001).
  - [4] K. Hinzer, M. Bayer, J. P. McCaffrey, P. Hawrylak, M. Korkusinski, O. Stern, Z. R. Wasilewski, S. Fafard, and A. Forchel, *Phys. Stat. Sol. (b)* **224**, 385 (2001).
  - [5] M. Bayer, G. Ortner, A. Larionov, V. Timofeev, A. Forchel, P. Hawrylak, K. Hinzer, M. Korkusinski, S. Fafard, and Z. Wasilewski, *Physica E* **12**, 900 (2002).
  - [6] G. Bester, J. Shumway, and A. Zunger, *Phys. Rev. Lett.* **93**, 47401 (2004).
  - [7] P. W. Fry, I. E. Itskevich, D. J. Mowbray, M. S. Skolnick, J. J. Finley, J. A. Barker, E. P. O'Reilly, L. R. Wilson, I. A. Larkin, P. A. Maksym, et al., *Phys. Rev. Lett.* **84**, 733 (2000).
  - [8] I. Shtrichman, C. Metzner, B. D. Gerardot, W. Y. Schoenfeld, and P. M. Petroff, *Phys. Rev. B* **65** (2002).
  - [9] M. Sugisaki, H. W. Ren, S. V. Nair, K. Nishi, and Y. Masumoto, *Physical Review B* **66** (2002).
  - [10] B. Alen, F. Bickel, K. Karrai, R. Warburton, and P. Petroff, *Appl. Phys. Lett.* **83**, 2235 (2003).
  - [11] A. J. Williamson, L.-W. Wang, and A. Zunger, *Phys. Rev. B* **62**, 12963 (2000).
  - [12] P. N. Keating, *Phys. Rev.* **145**, 637 (1966).
  - [13] L.-W. Wang and A. Zunger, *Phys. Rev. B* **59**, 15806 (1999).
  - [14] A. Szabo and N. S. Ostlund, *Modern Quantum Chemistry* (McGraw-Hill, New York, 1989).
  - [15] A. Franceschetti, H. Fu, L.-W. Wang, and A. Zunger, *Phys. Rev. B* **60**, 1819 (1999).
  - [16] R. Resta, *Phys. Rev. B* **16**, 2717 (1977).
  - [17] C. Bennett, H. Bernstein, S. Popescu, and B. Shumacher, *Phys. Rev. A* **53**, 2046 (1996).
  - [18] G. Bester, A. Zunger, and J. Shumway, *Phys. Rev. B* **??**, ??? (2005).
  - [19] L. He, G. Bester, and A. Zunger, *Phys. Rev. B* **??**, ??? (2005).
  - [20] C. Edmiston and K. Ruedenberg, *Rev. Mod. Phys.* **35**, 457 (1963).
  - [21] D. P. Craig and S. H. Walmsley, *Excitons in molecular crystals* (W. A. Benjamin, INC., New York, 1968).